DISCRETE ASIAN BARRIER OPTIONS

R. ZVAN*, P.A. FORSYTH† AND K.R. VETZAL‡

Abstract. A partial differential equation method based on using auxiliary variables is described for pricing discretely monitored Asian options with or without barrier features. The barrier provisions can be applied to either the underlying asset or to the average. They may also be of either instantaneous or delayed effect (i.e. Parisian style). Numerical examples demonstrate that this method can be used for pricing floating strike, fixed strike, American, or European options. In addition, examples are provided which indicate that an upstream biased quadratic interpolation is superior to linear interpolation for handling the jump conditions at observation dates. Moreover, it is shown that defining the auxiliary variable as the average rather than the running sum is more rapidly convergent for American-Asian options.

Keywords: Asian options, Barrier options, Parisian options, PDE option pricing
Running Title: Discrete Asian Barrier Options
Acknowledgment: This work was supported by the National Sciences and Engineering Research Council of Canada, the Social Sciences and Humanities Research Council of Canada, the Information Technology Research Center, funded by the Province of Ontario, and the Centre for Advanced Studies in Finance at the University of Waterloo.
AMS Classification: 65N30
Last Revised: December 3, 1998

Contact Address:
Peter A. Forsyth
Department of Computer Science
University of Waterloo
Waterloo Ontario N2L 3G1
paforsyt@yoho.uwaterloo.ca
Tel: (519) 888-4567 x4415

* Department of Computer Science, University of Waterloo, Waterloo, Ontario, Canada N2L 3G1, rzvan@yoho.uwaterloo.ca
† Department of Computer Science, University of Waterloo, paforsyt@yoho.uwaterloo.ca
‡ Centre for Advanced Studies in Finance, University of Waterloo, kvetzal@watarts.uwaterloo.ca

1. Introduction. Options having a payoff which depends on the average of the underlying asset are termed Asian options. Typically the average is arithmetic, but it is also possible to have a geometric average. In this article we consider only cases with arithmetic averages. Asian options are especially useful in cases where the underlying asset is foreign exchange or a commodity such as oil or aluminum. A corporation wishing to hedge a series of cash flows during some period may find that Asian options are a better choice than standard options [20]. Moreover, the use of an average price reduces the sensitivity of the option to price changes in the underlying asset near maturity [22]. There is considerable interest in developing methods for pricing both European and American Asian options (see, e.g. [23, 21, 30, 4, 38, 9, 3, 15] among others). There is also a rapidly expanding literature on the valuation of barrier options. See [6, 29, 12, 39, 8, 31] and references therein. If the purchaser of an option believes that it is very unlikely that the underlying asset will trade outside of a certain range, then barrier options can be viewed as inexpensive alternatives to regular options.

Standard knock-out options, where the option ceases to exist if the asset price breaches a barrier, are known to be difficult to hedge near the barrier [16]. As well, it has been suggested that traders may attempt to drive the asset price over a barrier so as to trigger knock-out [25]. In order to alleviate these problems, Parisian options [11, 10] have been suggested where knock-out (or knock-in) only occurs if the price of the asset remains continuously over the barrier for a specified length of time. A natural extension of an Asian option is an Asian-Parisian option. In this case. the payoff is depends on the average value, but a knock-out or knock-in provision is determined by a Parisian type barrier on the asset price [36]. A more recent alternative to Parisian options are step options, where the option loses value for each day over the barrier [25, 26, 14].

The objective of this article is to develop effective general-purpose numerical methods for pricing Asian options with barriers. In certain special cases, the Asian option pricing problem can be simplified through the use of transformations [35, 30, 3]. As our main objective is generality, we avoid transformations and make as few assumptions as possible about the form of the underlying process and the payoff. We believe that the techniques demonstrated in this article can be applied with only minor modifications to many different kinds of problems which may arise in practice. Both standard discrete and Parisian barriers will be considered. We assume that monitoring, both for the purposes of average calculation and barrier observation, is carried out discretely. Our method is quite general, in that any of the following can be specified:

- fixed or floating strike payoffs;
- early exercise;
- discrete dollar dividends or a continuous dividend yield;
- Parisian or standard discrete barriers, based on an asset value or an average value;
- irregularly spaced monitoring intervals;
- a CEV [13] process for the underlying asset, which of course includes the usual geometric Brownian motion process as a special case.

We use a discretized partial differential equation (PDE) approach, similar to that described in [17, 28, 15]. The auxiliary path-dependent variable advocated in this paper is the average, not the running sum as suggested in [17, 28]. We give numerical examples to indicate why we believe that the average is a better choice. In addition, our method of imposing early exercise constraints differs from that in [15]. Numerical examples are also given to demonstrate the methods on a wide variety of problems. We also explore the effect of the observation frequency on the convergence to the continuously monitored solution and show the impact of various types of barriers on the delta and gamma of the option.

2. Formulation. In the following, we will consider options which are functions of the price of an underlying asset S as well as possibly two path-dependent parameters. In particular, we consider options where the path-dependent parameters are the arithmetic average A of the underlying asset price and the number of successive observations J of either the asset or the average above or below a barrier. This will allow us to price Asian-Parisian options [36]. Since most (if not all) contracts feature discrete monitoring, we will consider only this case.

Let A_n be the discrete average obtained by sampling the asset at n monitoring times $t_1, t_2, \ldots, t_n$

$$A_n = \frac{\sum_{i=1}^{n} S_i}{n} \tag{1}$$

where $S_i = S(t_i)$. The average A_n can be computed recursively *viz*

$$A_n = A_{n-1} + \frac{S_n - A_{n-1}}{n} \tag{2}$$

where from (1) $A_1 = S_1$. If t_n is the n-th sampling date, let

$$\begin{aligned} t^+ &= t_n + \epsilon \\ t^- &= t_n - \epsilon \end{aligned} \tag{3}$$

where $\epsilon > 0$, $\epsilon \to 0$. Equation (2) can then be written as

$$A(S, t^+) = A(S, t^-) + \frac{S - A(S, t^-)}{n} \tag{4}$$

where $S = S(t_n)$, i.e. the current asset price at this sampling time. Equation (4) gives the jump in the discretely sampled average in terms of the asset price at the current observation time and the previous average.

In the Parisian case, we can also determine jump conditions for the counter J analogous to equation (4). Recall that J represents the number of successive observations that the asset is above (or below) a barrier. A Parisian up-and-out option, for example, ceases to have value if S is above the barrier for J^* successive observations. In the case of an up-and-in or up-and-out Parisian option, with a barrier given in terms of an asset price S^*,

$$J(S, t^+) = \begin{cases} \min(J(S, t^-) + 1, J^*) & S \geq S^* \\ 0 & S < S^* \end{cases} . \tag{5}$$

The cases of down-and-in and down-and-out contracts can be defined in an obvious manner. A detailed discussion of these conditions is given in [34]. It is also possible to define the barrier in terms of the average. In this case, we would modify equation (5) to

$$J(S, A, t^+) = \begin{cases} \min(J(S, A, t^-) + 1, J^*) & A \geq A^* \\ 0 & A < A^* \end{cases} \tag{6}$$

where A^* is the specified average barrier. If the average and barrier sampling times are coincident, then it is necessary to specify the precise order of average and barrier observation. For example, a contract could specify that the average is incremented first (equation (4)), and then the barrier is observed (equation (6)).

Consider an underlying asset with price S which evolves according to a constant elasticity of variance (CEV) process [13]:

$$dS = \mu S dt + \sigma S^{\alpha/2} dz \tag{7}$$

where μ is expected growth rate of the stock price, σ is the volatility, α is a parameter ($\alpha \geq 0$), and z is a Wiener process. Some further details on properties of CEV processes may be found in [1]. Note that if $\alpha = 2$ in equation (7), this is simply geometric Brownian motion. The usual no-arbitrage arguments then imply that the price of a derivative security $U = U(S, A, J, t)$ at time t which is not an observation time t_i is given by

$$U_t + \frac{\sigma^2 S^\alpha}{2} U_{SS} + rSU_S - rU = 0 \tag{8}$$

where r is the risk free rate of interest. Across sampling dates, absence of arbitrage also implies that the price of the option is continuous [35]. Consequently, around sampling dates we have the general jump condition

$$U(S, A^+, J^+, t^+) = U(S, A^-, J^-, t^-). \tag{9}$$

Details of the particular components of this condition are given by equations (4, 5, 6).

Discrete fixed dollar dividends are easily handled. If t^- and t^+ represent the times just before and after the ex-dividend dates, then for a European option

$$U(S, A, J, t^+) = U(S - D^*, A, J, t^-) \tag{10}$$

where D is the dividend payment and

$$D^* = \min(D, S). \tag{11}$$

Equation (11) prevents the unrealistic phenomenon of dividend payments being larger than the asset price. The value of $U(S - D^*, A, J, t^+)$ is calculated using linear interpolation. For an American option, equation (10) is modified to handle the possibility of early exercise. The case of a continuous dividend yield can of course be dealt with in the usual way.

3. Payoff and Boundary Conditions. Equation (8) is solved backward in time from the expiry date of the option $t = T$ to the present time $t = 0$, with jump condition (9) being applied at sampling times.

Consider first the initial conditions at $t = T$, $\forall S$, $\forall A$. For a knock-in option, these are

$$\begin{aligned} U(S, A, J = J^*, t = T) &= \text{usual Asian payoff} \\ U(S, A, J \neq J^*, t = T) &= 0 \end{aligned} \tag{12}$$

and for a knock-out option

$$\begin{aligned} U(S, A, J = J^*, t = T) &= 0 \\ U(S, A, J \neq J^*, t = T) &= \text{usual Asian payoff} . \end{aligned} \tag{13}$$

At times $t < T$ where $J \neq J^*$, we simply solve equation (8), imposing condition (9) at observation times, with suitable boundary conditions on $A \to \infty$, $S \to \infty$ (to be discussed below). At times $t < T$ with $J = J^*$, for a knock-out option the boundary condition is the Dirichlet condition $U = 0$. For a knock-in option, equation (8) is solved.

At points in equations (12, 13) where the payoff is given as the *usual Asian payoff*, we consider two types of payoffs at $t = T$. For a fixed strike (K), we have

$$U(S, A, J, t = T) = \begin{cases} \max(A - K, 0) & \text{for a call} \\ \max(K - A, 0) & \text{for a put} \end{cases} . \tag{14}$$

For a floating strike, we have

$$U(S, A, J, t = T) = \begin{cases} \max(S - A, 0) & \text{for a call} \\ \max(A - S, 0) & \text{for a put} \end{cases} . \tag{15}$$

Equation (8) normally requires boundary conditions at $S = 0$, $S \to \infty$. However, no condition is required at $S = 0$ since all of the spatial derivative terms vanish there (this implicitly assumes $\alpha > 0$; if $\alpha = 0$ then a boundary condition would have to be imposed). For a fixed strike, as $S \to \infty$ the boundary condition is initially set to the payoff condition. At observation times, the Dirichlet condition at $S \to \infty$ is reset according to equation (9). For a floating strike, the boundary conditions at $S \to \infty$ are also set initially to the payoff condition. For all points $S \neq A$, these conditions are reset at observation times using equation (9). At $S = A \to \infty$, we take the condition to be

$$U(S = \infty, A = \infty, J, t < T) \simeq \beta S \tag{16}$$

for some $\beta = \beta(t)$. This can be derived assuming that the solution to the PDE problem can be written as

$$A\beta(S/A) \tag{17}$$

for some β and for a fixed value of J, which is the case for $\alpha = 2$. This condition is not precisely correct if $\alpha \neq 2$, but numerical tests show that the precise form of the boundary condition at $S = A \to \infty$ is not very important as long as $S_{max} = A_{max}$ is large.

4. Numerical Algorithm. Away from observation times, equation (8) has no A or J dependence. Consequently, this means that a set of independent one-dimensional PDE problems can be solved for each specified A and J. This type of approach has been suggested in [35, 17, 28, 15] for Asian options, although a path-dependent state variable in terms of the running sum instead of the average was used in [35, 17, 28].

An obvious implementation was used here: a class was developed which could solve the one-dimensional PDE problem (8). Asian options can be regarded as a collection of these one-dimensional objects. Each object is associated with a given value of A. Asian-Parisian options can then be regarded as a collection of Asian objects, each Asian object being associated with a given value of J. This approach can clearly be extended to include more path-dependent variables, but at increased computational cost.

The one-dimensional problems were solved using a finite volume method with non-uniform node spacing, as in described in [38]. In the case of American options, the penalty method outlined in [37] was used. In this approach the early exercise condition results in a set of nonlinear algebraic equations. These are solved using Newton iteration. As well, our one-dimensional PDE solver automatically detects when the problem is convection dominated [38] and switches from a standard central difference to a high order flux limited scheme [32]. Consequently, it is always assumed that the discrete equations are nonlinear and that Newton iteration is required. The Jacobian is constructed using numerical differentiation.

Since the equations are assumed nonlinear, at least two nonlinear iterations are required per timestep. For the European option examples presented in this work, with typical values for σ, r, and α, this is completely unnecessary since the discrete equations are linear. However, in order to make a *fair* comparison with the American option examples, we make no assumptions about the linearity of the discrete equations. Consequently, the CPU time results for the European examples presented here are at least double that which would be required if we forced only one nonlinear iteration per timestep. The convergence tolerance for the nonlinear iteration (at node i, timestep $n+1$) is

$$tol = \max(10^{-5}, U_i^{n+1} \times 10^{-5}). \tag{18}$$

Conceptually, this problem can be considered to be a collection of one-dimensional PDE's, embedded in a higher (in this case two or three) dimensional space. Communication between these independent one-dimensional problems only occurs at observation times. Clearly, this approach is ideally suited to an implementation on parallel architectures, although we will not pursue this idea further in this work.

At each observation time the jump condition (9) is applied. This generally involves some form of interpolation. However, in the case of Parisian options interpolation in the J direction is often not required. This is because J^* is typically small, e.g. 10 to 20. In this case $J^* + 1$ Asian objects (corresponding to values of $J = 0, 1, \ldots, J^*$) are required to avoid any interpolation.

The situation is a bit more complicated for interpolation in the A direction. One possibility is to simply use linear interpolation, as suggested in [21, 4]. However, as we shall demonstrate, a higher order interpolant is preferable. To motivate our discussion of this point, consider an Asian option where the average is computed continuously,

$$A = \frac{\int_0^t S(t')\, dt'}{t}. \tag{19}$$

For simplicity, we ignore any barrier features. In this case, the value of an Asian option is $U = U(S, A, t)$ [4] where U satisfies:

$$U_t + \frac{\sigma^2 S^\alpha}{2} U_{SS} + rSU_S + \frac{1}{t}(S - A)U_A - rU = 0. \tag{20}$$

A more standard form for equation (20) can be obtained by letting $\tau = T - t$, so that equation (20) becomes:

$$U_\tau - \frac{1}{T-\tau}(S - A)U_A = \frac{\sigma^2 S^\alpha}{2} U_{SS} + rSU_S - rU. \tag{21}$$

This equation has the familiar form of a convection-diffusion equation. Note that the convective term has a velocity in the A direction given by

$$-\frac{1}{T-\tau}(S - A). \tag{22}$$

In other words, the information flow (from this term) is from the diagonal of the grid ($S = A$) outward in the A direction. We can regard discrete averaging as being the limit as the term (22) becomes very large (i.e. a delta function) near the sampling dates. In this case, the continuous problem becomes a convection dominated PDE [38], and special care has to be taken with handling the first order hyperbolic term in equation (20).

By analogy with high order limiter methods [2, 18, 38], we will use an limited quadratic upstream biased interpolation method. For ease of exposition, consider the case of a tensor product grid where the coordinates of node (i, j) are (S_i, A_j). Again, if we view the discrete averaging problem as the limiting case of a continuous average, then the upstream node (at the sampling date) for any point (S_i, A) is the node (S_i, A_{ups}) closer to the diagonal ($A = S_i$). Suppose that the jump condition (9) requires a value of $U = U(S_i, A')$ at point A' which is not a grid point A_j. If

$$A_j \le A' \le A_{j+1}, \tag{23}$$

then

$$\begin{aligned}
j_{up} &= \begin{cases} j+1 & A' < S_i \\ j & A' > S_i \end{cases} \\
j_{down} &= j + (j+1) - j_{up} \\
j_{2up} &= \begin{cases} j+2 & A' < S_i \\ j-1 & A' > S_i \end{cases}
\end{aligned} \tag{24}$$

FIG. 1. *Locations of interpolated data (S, A^+) at observation dates for cases where $S > A$ and $S < A$. Note that information from the solution at time just after the observation time flows outward from the diagonal of the grid to the solution just before the observation time (recall the PDE is being solved backward in time).*

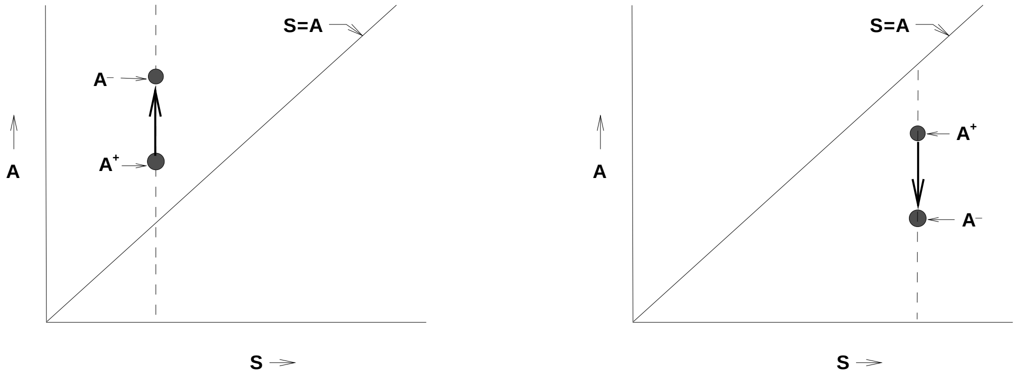

where j_{up}, j_{down}, and j_{2up} are the upstream, downstream, and second upstream points respectively [33]. The value of $U(S_i, A')$ is then estimated using quadratic Lagrange interpolation using data at the points (i, j), (i, j_{up}), (i, j_{2up}). The interpolation is limited to suppress oscillations [24]

$$\begin{aligned} U(S_i, A') &\leq \max\left[U\left(S_i, A_{j_{up}}\right), U\left(S_i, A_{j_{down}}\right)\right] \\ U(S_i, A') &\geq \min\left[U\left(S_i, A_{j_{up}}\right), U\left(S_i, A_{j_{down}}\right)\right]. \end{aligned} \tag{25}$$

This approach is similar to MUSCL methods [2]. Note that if $A_{j_{2up}} > S_i$ and $A' < S_i$ or $A_{j_{2up}} < S_i$ and $A' > S_i$, then linear interpolation is used. This is because interpolation should not be used across the $S = A$ line (the *velocity* in equation (22) changes sign at $S = A$). We also assume that there is always a node in the mesh where $A_j = S_i$.

We illustrate the interpolation procedure at observation dates in Figure 1. Given a value of (S, A^-), the figure shows typical locations for (S, A^+) (recall we are solving the PDE backward in time), where the values for U are obtained using interpolation. Note that information *flows* in different directions, depending on whether $S < A$ or $S > A$.

5. Quadratic Interpolation for the Average. In order to demonstrate the benefits of quadratic interpolation, we consider Asian options without any barrier provisions. In this case, the discrete Asian option pricing problem requires solution of a set of one-dimensional PDE's embedded in a two-dimensional space.

The jump conditions for the n-th average observation are (at $t = t_n$)

$$\begin{aligned} U(S, A^+, t^+) &= U(S, A^-, t^-) \\ A^+ &= A^- + \frac{S - A^-}{n}. \end{aligned} \tag{26}$$

TABLE 1

Convergence of quadratic and linear interpolation, American floating strike put, $T - t = .25$, observation frequency $= .004$, timestep $= .004$, $r = .10$, $\alpha = 2$. Time units are years. Value of option at $S = \$100$.

Floating Strike American-Asian Put Option				
	$\sigma = .2$		$\sigma = .4$	
Grid Size	Linear	Quadratic	Linear	Quadratic
37×37	2.9668	2.9221	6.4068	6.3281
73×73	2.9378	2.9133	6.3370	6.2852
145×145	2.9231	2.9138	6.3027	6.2814
289×289	2.9177	2.9145	6.2878	6.2807

Table 1 compares the use of linear and quadratic interpolation for enforcing condition (26) for an American floating strike put (complete data is given in the caption of the table). A fixed timestep of one day (1/250 year) was used, so that the changes in the solution in Table 1 are due to spatial discretization error. Crank-Nicolson timestepping was employed. The coarsest grid used a non-uniform spacing in the S direction (37 nodes) with $\Delta S = .5$ near the value of $S = 100$. The same mesh spacing was used in the A direction resulting in a 37×37 grid. Finer meshes were constructed by inserting a new node between each two coarse mesh nodes in both the S and A directions. Table 1 clearly demonstrates that use of the upstream biased quadratic interpolation described in the previous section converges more rapidly as the mesh is refined compared to linear interpolation. Quadratic interpolation will be used for all subsequent examples. Note that since convergence criterion (18) was used for these examples, the fifth figure in Table 1 should be viewed with caution.

6. Comparison with Running Sum Formulation. As an alternative to using the average as the auxiliary variable, the running sum

$$I_n = \sum_{i=1}^{n} S_i \tag{27}$$

has been suggested in [17, 35, 28]. In this case, the jump conditions at a sampling date are

$$\begin{aligned} U(S, I^+, t^+) &= U(S, I^-, t^-) \\ & \quad I^+ = I^- + S. \end{aligned} \tag{28}$$

Let N be the total number of observation times. Then the payoff conditions for a fixed strike are

$$U(S, I, t = T) = \begin{cases} \max(I/N - K, 0) & \text{for a call} \\ \max(K - I/N, 0) & \text{for a put} \end{cases}, \tag{29}$$

while for a floating strike we have

$$U(S, I, t = T) = \begin{cases} \max(S - I/N, 0) & \text{for a call} \\ \max(I/N - S, 0) & \text{for a put} \end{cases}. \tag{30}$$

FIG. 2. *Value of a floating strike Asian put computed using the running sum formulation, with* $\sigma = .4$, $T - t = .25$, $r = .1$, $\alpha = 2$. *Asian observation frequency* $= .001$, *timestep size* $= .001$. $S_{max} = 300$, $I_{max} = 25200$, $\Delta S = .5$, $\Delta I = 50$. *Domain in the* I *direction should extend to* $(N+1) \times S_{max} = 75600$ *to avoid extrapolation. Note that the solution should be a straight line.*

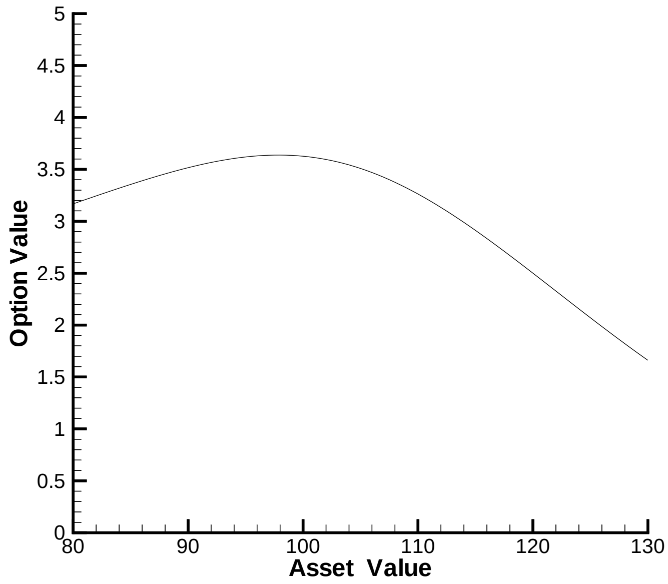

From the jump conditions (28) it is immediately obvious that the value of the option at $U(S, I = 0, t = 0)$ depends on values of I up to $I = S_{max} \times (N + 1)$, where S_{max} is the maximum value of S. In [28] it was suggested that the domain could be truncated in the I direction, and that the missing I values could be determined by extrapolation. While this may be reasonable for fixed strike problems, it is not advisable for floating strike payoffs. Figure 2 shows the value of a floating strike Asian put computed using the running sum formulation (Crank-Nicolson timestepping was used for all examples in this section). In this case, since $S_{max} = 300$ and there are 251 sampling dates, the domain in the I direction should extend to $I_{max} = 75600$. For this example, the I domain is truncated at $I_{max} = 25200$. Any missing data is determined by extrapolation. If interpolation is required for the jump condition (28), upstream biased quadratic interpolation is used.

The solution to the floating strike PDE with $\alpha = 2$ can be written as $IG(S/I)$ for some function G. As a result, the solution at $t = 0$ where $S = I$ should be a straight line. This is clearly not the case in Figure 2. This problem disappears if the domain in the I direction is extended to $I = S_{max} \times (N+1)$, indicating that, in general, extrapolation of missing data is undesirable.

If we use a value of $I_{max} = S_{max} \times (N+1)$ and specify the same number of nodes in the I and S directions (with constant mesh spacing in both directions), then the node spacing in the I direction will be $\Delta I = (N + 1) \times \Delta S$ (as in the example presented in [28]). Table 2 compares the use of the running sum formulation with the average

TABLE 2

Comparison of running sum and average formulation for a fixed strike Asian call option. $\sigma = .4$, $T - t = .25$, $r = .1$, $K = 100$, $\alpha = 2$, value of option at $S = 100$. Asian observation frequency = .004, timestep size = .004. The average formulation used equal grid spacing in A and S directions. The running sum formulation used the same number of nodes in the I and S direction, with equal spacing in each direction. As well, we give results for the solution obtained using the average formulation with a variably spaced mesh. These grids used a fine spacing near $S = 100$.

Fixed Strike Asian Call Option				
	European		American	
Grid Size	Running Sum	Average	Running Sum	Average
constant mesh spacing				
150×150	5.082	5.133	13.354	5.832
300×300	5.106	5.127	11.589	5.796
600×600	5.109	5.126	7.671	5.789
variable mesh spacing				
73×73		5.117		5.775
145×145		5.123		5.784
289×289		5.124		5.787

formulation. To provide a fair comparison, a constant grid spacing $\Delta S = \Delta A$ was used for the average formulation. We also present results using a finer mesh near the desired value of S which demonstrate that it is more efficient to use non-uniform grids. For the running sum formulation, we used a constant spacing determined by dividing I_{max} and S_{max} by the total number of nodes in that direction. This produces exactly the same mesh spacing in the S direction for both formulations. For the European example, both methods give comparable results for the same number of nodes. However, for the American option the running sum formulation gives very poor convergence relative to the average formulation. If a very fine grid spacing is used in the I direction, then the running sum prices are close to the average formulation prices, but only with a much larger number of nodes.

Of course, we have not demonstrated that there is not some choice of mesh spacing in the I direction for which the running sum method will give convergence comparable to the average formulation with the same number of nodes. However, we were unable to improve the results significantly after numerous attempts. Moreover, note that a given average is a fixed line in the $S \times A$ grid, whereas it is given by I/N in the running sum formulation. As a result, it is a simple matter in the average formulation to use a fine mesh spacing near a given average value (e.g. a barrier based on the average), but this is not the case for the running sum formulation. Consequently, since it would appear that the average formulation offers several advantages compared to the running sum method, we will use this formulation exclusively in the remainder of this article.

7. Convergence: Analysis. A detailed analysis of the convergence of discretely observed lattice and PDE methods for Asian option is given in [19]. In this section, we give a brief summary of the convergence estimates for the PDE method.

If Crank-Nicolson timestepping is used, and a second order space discretization, then we can expect that the discretization error for the one-dimensional PDE's will be

$$\text{discretization error} = O\left((\Delta S)^2\right) + O\left((\Delta t)^2\right) \tag{31}$$

where ΔS is the maximum grid spacing in the S direction.

In addition to the usual PDE discretization errors, there will also be an interpolation error at each discrete observation, due to condition (9). Since a stable method is being used to solve the PDE, these errors do not become amplified but in the worst case will accumulate. If we assume that quadratic interpolation is used, then the interpolation error at each observation will be

$$\text{interpolation error at each observation} = O\left((\Delta A)^3\right) \tag{32}$$

where ΔA is the maximum grid spacing in the A direction. If the interval between observations is Δt_{obs}, after $O(1/(\Delta t_{obs}))$ observations the cumulative interpolation error will be

$$\text{cumulative interpolation error} = O\left(\frac{(\Delta A)^3}{\Delta t_{obs}}\right). \tag{33}$$

In addition, there will also be an error if we are attempting to converge to the continuous time limit using a discretely observed model. This error will be

$$\text{error in discrete observation} = O(\Delta t_{obs}). \tag{34}$$

In general, the error in a PDE method will be the sum of all these errors. Note that it is not possible to let $\Delta t_{obs} \rightarrow 0$ with a fixed grid size, since equation (33) becomes unbounded. Suppose that convergence to the continuously observed limit is desired. If $\Delta A = \Delta S = C\Delta t_{obs}$ (where C is a constant), convergence will be attained. In this case, the discrete observation error (34) will dominate and the convergence will be $O(\Delta t_{obs})$.

On the other hand, discrete observation (often daily) is specified in most contracts. In this case, as long as $\Delta t \leq \Delta t_{obs}$, then error (34) is no longer present, and the interpolation error (33) does not become unbounded (since Δt_{obs} is fixed). Consequently second order convergence can be expected. In practice, the time truncation error is usually very small (e.g. if the observation interval and the timestep are each one day), so that the error is dominated by the spatial discretization error.

8. Convergence of Discrete Asian Options to Continuous Limit: Numerical Results. Tables 3, 4, 5 and 6 show the effect of mesh size and timestep size on the convergence of the discretely observed Asian option (without any barrier provisions) to a continuously observed limit, for European and American options with both floating and fixed strike payoffs. These particular pricing problems were investigated in [4] and [38], using a variety of continuously observed models (including a two-dimensional PDE approach, the forward shooting grid method developed in [4], and, for European options, the one-dimensional PDE derived in [30]). Some of these same problems have also been addressed in [15] using LP methods. For comparative purposes, our tables

TABLE 3

Convergence of a discrete fixed strike European-Asian call option to the continuous time limit. $T - t = .25$, $K = \$100$, $r = .10$, $\alpha = 2$. Time units are years. CPU time for a Pentium-Pro 200 Mhz PC.

Fixed Strike European-Asian Call Option						
			$\sigma = .2$		$\sigma = .4$	
Grid Size	Observation frequency	Timestep	Value ($S = 100$)	CPU (sec) (P-200)	Value ($S = 100$)	CPU (sec) (P-200)
37×37	.004	.004	2.8961	3.6	5.0948	3.5
	.004	.002	2.8960	5.5	5.0947	5.5
	.002	.002	2.9151	7.2	5.1268	7.1
	.001	.001	2.9173	14.5	5.1313	14
73×73	.002	.002	2.9242	22.9	5.1493	22.5
	.001	.001	2.9264	44.1	5.1537	43
145×145	.001	.001	2.9287	162	5.1597	161
289×289	.001	.001	2.9293	710	5.1613	712
	Maximum in [38]		2.960		5.218	
	Minimum in [38]		2.923		5.164	

here provide the highest and lowest values of the corresponding estimates reported in [38] from these various alternative methods. It should be pointed out that the results in [38] are for daily timesteps and fairly coarse grids. As such they are better viewed as ballpark estimates than converged answers. Also, note that the PDE for a floating strike option without discrete dollar dividends and with $\alpha = 2$ in equation (7) can be reduced to a one-dimensional PDE through use of a similarity transformation [35], so we include this case simply as a demonstration of the numerical method.

Our calculations assume that there are 250 days in a year, so that an observation frequency or timestep size of .004 corresponds to one day. As a rough check, in almost all of the cases our answers with a fine grid and small timestep size and observation interval are quite close to the estimates from [38]. The only exception is for a floating strike American put option when $\sigma = .4$ in Table 6. Our converged answer using a fine grid with quarter-day (.001) observations and timesteps was $\simeq \$6.21$, somewhat above the range of \$6.00-\$6.11 from [38]. It is worth noting that a value of \$6.18 is reported in [15] for this problem. This figure is based on a much finer grid and smaller timestep size than the estimates from [38]. It is therefore reasonable to conclude that the estimates in [38] are not very precise in this instance. This particular case also reveals an interesting phenomenon. A converged estimate of the value of this option under daily observation and timesteps is available from Table 1 and it is $\simeq \$6.28$ (the time truncation error was negligible for these runs). This shows that, in some circumstances at least, increasing the observation frequency from daily to a higher frequency such as four times per day can have a noticeable effect on the value of an Asian option. It also suggests that a continuously observed model may potentially produce inaccurate values of a discretely (e.g. daily) monitored Asian option.

It is also interesting to observe that all of the cases show very little time truncation

Table 4

Convergence of a discrete fixed strike American-Asian call option to the continuous time limit. $T - t = .25$, $K =$ \$100, $r = .10$, $\alpha = 2$. Time units are years. CPU time for a Pentium-Pro 200 Mhz PC.

Fixed Strike American-Asian Call Option						
			$\sigma = .2$		$\sigma = .4$	
Grid Size	Observation frequency	Timestep	Value ($S = 100$)	CPU (sec) (P-200)	Value ($S = 100$)	CPU (sec) (P-200)
37×37	.004	.004	3.1843	3.8	5.7554	3.8
	.004	.002	3.1847	6.1	5.7565	6.1
	.002	.002	3.2047	7.3	5.7920	7.2
	.001	.001	3.2074	14	5.7984	14.2
73×73	.002	.002	3.2080	23.5	5.8095	23.5
	.001	.001	3.2104	46	5.8142	46
145×145	.001	.001	3.2127	168	5.8226	211
289×289	.001	.001	3.2134	714	5.8250	718
	Maximum in [38]		3.224		5.846	
	Minimum in [38]		3.219		5.826	

Table 5

Convergence of discrete floating strike European-Asian put option to the continuous time limit. $T - t = .25$, $r = .10$, $\alpha = 2$. Time units are years. CPU time for a Pentium-Pro 200 Mhz PC.

Floating Strike European-Asian Put Option						
			$\sigma = .2$		$\sigma = .4$	
Grid Size	Observation frequency	Timestep	Value ($S = 100$)	CPU (sec) (P-200)	Value ($S = 100$)	CPU (sec) (P-200)
37×37	.004	.004	1.6942	3.9	3.9133	4.4
	.004	.002	1.6942	5.8	3.9133	6
	.002	.002	1.6853	7.3	3.8916	7.7
	.001	.001	1.6876	14.5	3.8963	14
73×73	.002	.002	1.7015	23	3.9336	25
	.001	.001	1.7036	53	3.9379	47
145×145	.001	.001	1.7121	171	3.9585	176
289×289	.001	.001	1.7146	718	3.9653	722
	Maximum in [38]		1.724		3.981	
	Minimum in [38]		1.679		3.926	

TABLE 6

Convergence of discrete floating strike American-Asian put option to the continuous time limit. $T - t = .25$, $r = .10$, $\alpha = 2$. Time units are years. CPU time for a Pentium-Pro 200 Mhz PC.

Floating Strike American-Asian Put Option						
			$\sigma = .2$		$\sigma = .4$	
Grid Size	Observation frequency	Timestep	Value ($S = 100$)	CPU (sec) (P-200)	Value ($S = 100$)	CPU (sec) (P-200)
37×37	.004	.004	2.9221	4.1	6.3281	4.6
	.004	.002	2.9239	6.2	6.3287	6.6
	.002	.002	2.9066	7.5	6.2930	7.8
	.001	.001	2.8994	14	6.2779	14
73×73	.002	.002	2.8922	25	6.2414	26
	.001	.001	2.8818	50	6.2198	50
145×145	.001	.001	2.8797	175	6.2087	187
289×289	.001	.001	2.8794	712	6.2066	712
	Maximum in [38]		2.867		6.111	
	Minimum in [38]		2.773		5.996	

error with daily observation and daily timesteps (i.e. the solution values do not change appreciably if the timestep size is halved, holding the observation interval constant). An examination of spatial grid refinements when the observation frequency and timestep size are each .001 reveals that the computed values change by about a penny when $\sigma = .2$ and around 2-3 cents when $\sigma = .4$ going from the coarsest to the finest grid for fixed strike calls (Tables 3 and 4). The corresponding changes for the floating strike puts are in the neighborhood of 2 cents when $\sigma = .2$ and 6-7 cents when $\sigma = .4$ (Tables 5 and 6). The general implication is that the computational cost for pricing a continuously observed Asian option using a discretely observed model is highly dependent on the accuracy required (and somewhat dependent on the parameters of the problem). It is more expensive to achieve a given level of accuracy for floating strike puts than for fixed strike calls, or when σ is higher. The convergence analysis of the previous section indicates that our method will converge to the continuously observed limit only at the rate of $O(\Delta t_{obs})$. If continuously observed prices are actually required, then it may be more efficient to use a continuously observed model as in [38]. It is also worth mentioning that a comparison of Table 3 with Table 4 and of Table 5 with Table 6 shows that early exercise premia can be substantial for Asian options.

A study of convergence in a more practical case is shown in Table 7. In this case, the objective is to price a one year American-Asian fixed strike option with daily monitoring. This problem cannot be reduced to a one-dimensional PDE. As for the previous examples, reduction of the timestep to less than one day (but with daily observation) resulted in changes to the solution only in the fourth figure, and hence such results are not shown. Table 7 indicates that the solution on the finest 289×289 grid using daily timesteps and observations is accurate to within a penny. Required CPU time can be reduced by either using larger timesteps and hence less frequent observation intervals, or by using a coarser grid. In [4] an accuracy criterion of 0.1% of

TABLE 7
Comparison of various observation frequencies and grid size effects for an American-Asian fixed strike call option. $r = .10$, $T - t = 1.0$, $K = 100$, $\alpha = 2$. CPU time for a Pentium-Pro 200 Mhz PC. Time units are years. Timestep size = observation frequency.

Fixed Strike American-Asian Put Option					
		$\sigma = .2$		$\sigma = .4$	
Grid Size	Observation frequency (Δt)	Value ($S = 100$)	CPU (sec) (P-200)	Value ($S = 100$)	CPU (sec) (P-200)
37×37	.004	7.5177	14	12.452	14
	.01	7.5090	5.7	12.431	12
	.02	7.4958	3.4	12.398	4
73×73	.004	7.5250	46	12.470	45
	.01	7.5189	19	12.455	20
	.02	7.5092	12	12.433	15
145×145	.004	7.5340	171	12.491	171
	.01	7.5281	72	12.477	74
	.02	7.5185	50	12.456	61
289×289	.004	7.5366	685	12.498	694
	.01	7.5306	313	12.483	316
	.02	7.5207	231	12.463	286
Maximum in [38](continuous)		7.548		12.497	
Minimum in [38](continuous)		7.521		12.439	

S_0 was suggested. Prices to this level of accuracy can be obtained in $\simeq 4$ seconds. As noted earlier, for a European option this is an overestimate by a factor of at least two.

9. Discretely Monitored Barriers: Non-Parisian Case. For these examples, we assume that there is a barrier at $S = 120$ or $A = 120$ (strike $K = \$100$). These are the usual discretely observed knockout barriers, so that the Parisian path-dependent variable J (equation (5)) is not required. Consequently, this is a two-dimensional problem. In the following examples, we take the Asian observation times and the barrier observation times to be the same dates. To avoid any ambiguity, at each monitoring date, the Asian observation is carried out first and then the barrier observation.

As demonstrated in [40, 39], Crank-Nicolson timestepping can cause spurious oscillations for discretely observed barriers. Therefore we used a fully implicit method for these problems. A very small timestep $\simeq 10^{-5}$ years is used after each barrier observation, and then a timestep selector [39] is used to increase the timestep until the next monitoring date is reached.

Table 8 shows the results (price, delta = U_S, gamma = U_{SS}) for a 101×101 grid and a 201×201 grid for a fixed strike Asian call option with a discretely monitored knockout barrier at $S = 120$. A highly non-uniform grid was used with $\Delta S = .0025$ near the barrier. The same mesh spacing was used in both the A and S directions. Table 8 indicates that the solution is adequately resolved on the 101×101 mesh, so this grid and timestep sequence will be used for all subsequent examples.

Figure 3 compares the price for a fixed strike ($K = 100$) Asian call option with i)

TABLE 8

Convergence of discrete barrier fixed strike Asian call option. $\sigma = .25$, $T-t = .5$, $r = .05$, $K = 100$, $\alpha = 2$. *Asian observation frequency* $= 1/250$ *(1 day). Barrier observation frequency* $= 1/250$ *(1 day). Barrier at asset value* $= 120$. *The fine grid run also uses smaller timesteps.*

Grid Size	Quantity	$S = 100$	$S = 110$	$S = 120$
101×101	price	.84790	1.1961	0.19596
	delta	.077034	-0.032199	-0.11660
	gamma	-0.002510	-0.01640	0.03322
Smaller timesteps				
201×201	price	.84872	1.1971	0.19667
	delta	.077254	-0.032200	-0.11641
	gamma	-0.002509	-0.01642	0.03368

no barriers; ii) a discretely observed barrier at $S = 120$; and iii) a discretely observed barrier at $A = 120$. Intuitively, one would expect that it would be less probable that a barrier based on an average would be breached, and hence an option with a barrier based on the average should be more expensive than an option with a barrier based on the asset value. This is indeed the case. In fact, the average value barrier is considerably more expensive than the asset value barrier.

Figure 4 shows the price of options with various permutations of barrier applications. One possibility for softening the effect of the barrier is to allow no increase in the value of the computed average if the asset price is above the barrier value. This is in effect a type of ratchet barrier. More precisely, the average calculation becomes:

$$A^+ = \begin{cases} A^- + \dfrac{S - A^-}{N} & S < S^* \\ A^- & S \geq S^* \end{cases} \tag{35}$$

where S^* is the barrier location. Figure 4 shows that this ratchet barrier contract is actually less expensive than the Asian with an average barrier for asset prices less than $\simeq 100$. However, this is a fairly small effect, and the ratchet barrier becomes much more expensive than the average barrier for higher values of S.

The average is very sensitive to the observed price for the first few barrier observations. This sensitivity can be reduced by delaying the start of the barrier observation (but not the average observation). Figure 4 shows that the delayed barrier observation does indeed smooth the price near $S = 120$. However, it is interesting to note that the delayed average barrier and the usual average barrier give precisely the same price for asset values less than $\simeq 110$.

10. Asian-Parisian Barriers. Recently, Parisian options [11, 10, 36] have been suggested as a contract which reduces the possibility of market manipulation as the asset nears the barrier. Asian-Parisian options have been proposed in [36] as an appropriate implementation of a barrier for Asian options.

Recall that J^* is the critical number of successive observations above the barrier before knock-in or knock-out occurs. As noted previously, no interpolation is required

FIG. 3. *Comparison of fixed strike Asian call option with barrier on asset price and Asian option with barrier on the average asset price.* $\sigma = .25$, $T - t = .5$, $r = .05$, $K = 100$, $\alpha = 2$. *Asian observation frequency* $= 1/250$ *(1 day). Barrier observation frequency* $= 1/250$ *(1 day). Barrier at asset value* $= 120$ *or average value* $= 120$.

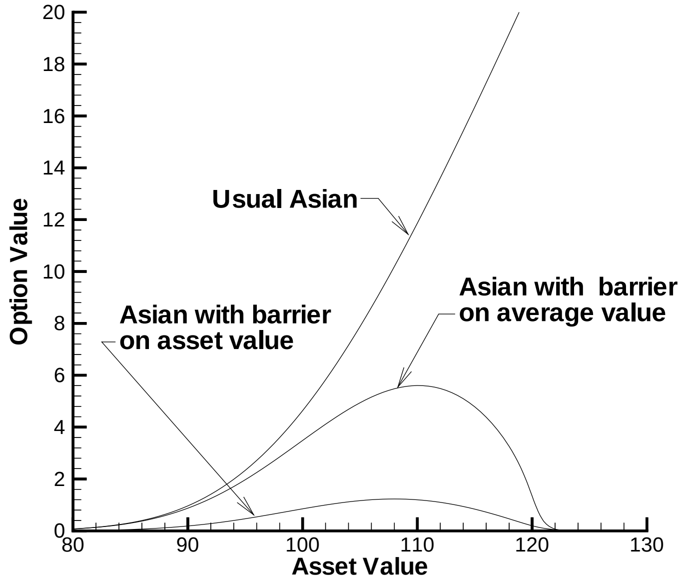

FIG. 4. *Comparison of fixed strike Asian call option with barrier on the average asset price, same with start of barrier observation delayed by .1 years, and barrier which does not allow an increase in the average when the asset price is over the barrier, as in equation (35).* $\sigma = .25$, $T - t = .5$, $r = .05$, $K = 100$, $\alpha = 2$. *Asian observation frequency* $= 1/250$ *(1 day). Barrier observation frequency* $= 1/250$ *(1 day). Barrier at asset value* $= 120$ *or average value* $= 120$.

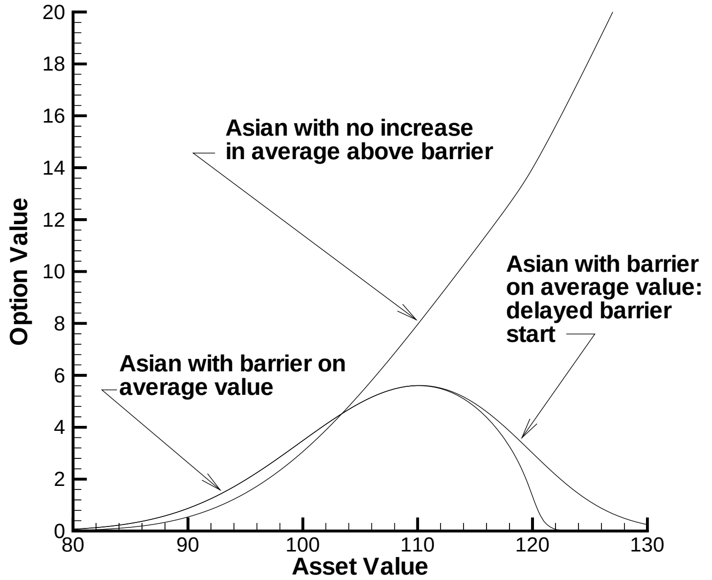

FIG. 5. *Comparison of fixed strike Asian call option with Parisian knock-out barrier for various values of J^*. $\sigma = .25$, $T - t = .5$, $r = .05$, $K = 100$, $\alpha = 2$. Asian observation frequency $= 1/250$ (1 day). Barrier observation frequency $= 1/250$ (1 day). Barrier at asset value $= 120$.*

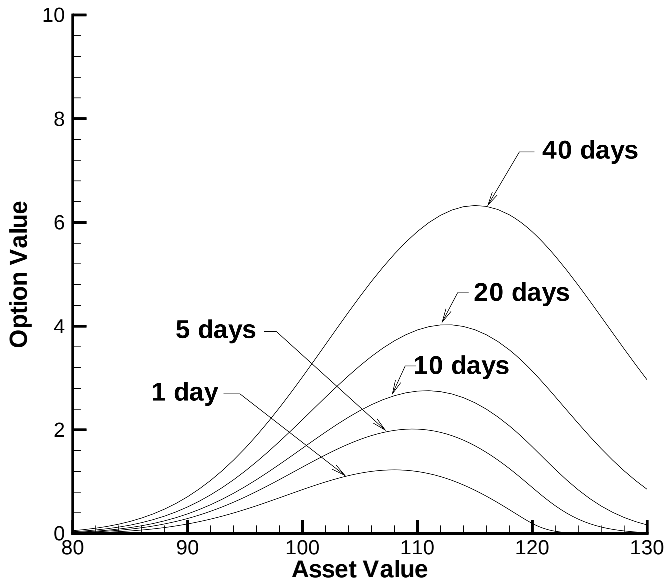

if there are $J^* + 1$ Asian objects used in the price computation for Asian-Parisian options. In other words, there is no discretization error in the J direction. Since there are now three space-like variables (S, A, J), we use a three-dimensional grid of size $101 \times 101 \times (J^* + 1)$, where the same $S \times A$ grid is employed as in Section 9. Again, to avoid ambiguity, at any monitoring date the Asian observation is carried out first and then the Parisian observation.

Figures 5 and 6 show the price, delta, and gamma for a fixed strike Asian call with a Parisian knock-out condition relative to $S = 120$. The results are given for various values of the number of continuous observations over the barrier before the knock-out is triggered (J^*). As expected, the price for $J^* = 40$ is much higher than the equivalent case with $J^* = 1$, which is effectively a typical discrete knock-out. Note also that maximum value of gamma is considerably reduced as J^* is increased. However, gamma takes on large negative values for the $J^* = 40$ contract, so hedging may not be much easier for this contract than for the $J^* = 1$ case.

An Asian-Parisian knock-in barrier where knock-in only occurs if the underlying price is above the barrier for a period of time represents a *worst case* hedge, i.e. when both the average and spot price are high [36]. Figures 7 and 8 show the price, delta, and gamma for fixed strike Asian call with a Parisian knock-in barrier. Clearly, if J^* (the number of observations before knock-in occurs) is large, then the option is significantly less valuable near $S = 100$ than the standard knock-in. It is not surprising that the plots for delta and gamma indicate that it is easier to hedge these contracts when J^* is relatively large.

FIG. 6. *Comparison of delta and gamma of a fixed strike Asian call option with a Parisian knock-out barrier for various values of* J^*. $\sigma = .25$, $T - t = .5$, $r = .05$, $K = 100$, $\alpha = 2$. *Asian observation frequency* = 1/250 *(1 day). Barrier observation frequency* = 1/250 *(1 day). Barrier at asset value* = 120.

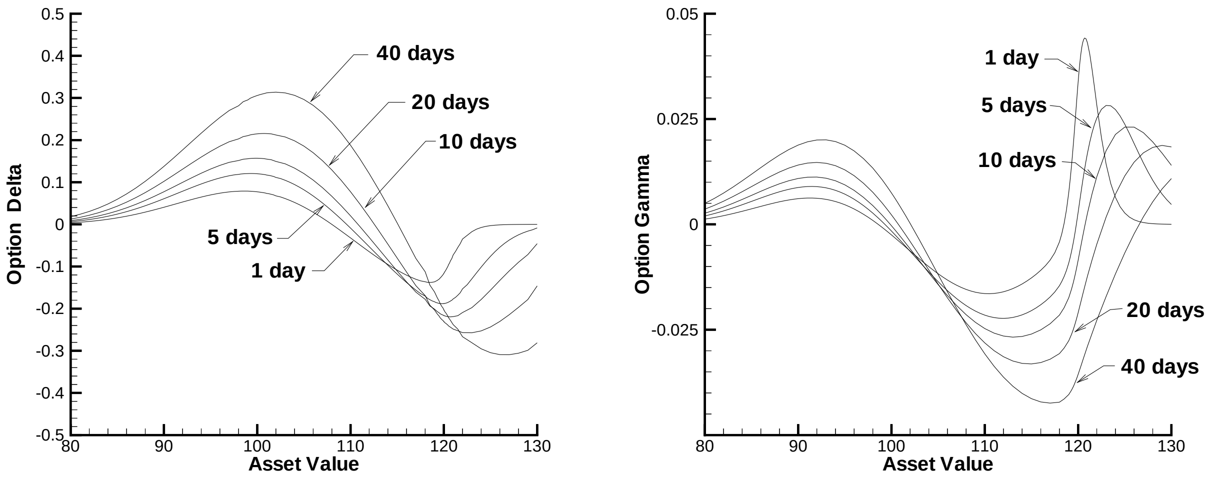

FIG. 7. *Comparison of a fixed strike Asian call option with Parisian knock-in barrier for various values of* J^*. $\sigma = .25$, $T - t = .5$, $r = .05$, $K = 100$, $\alpha = 2$. *Asian observation frequency* = 1/250 *(1 day). Barrier observation frequency* = 1/250 *(1 day). Barrier at asset value* = 120.

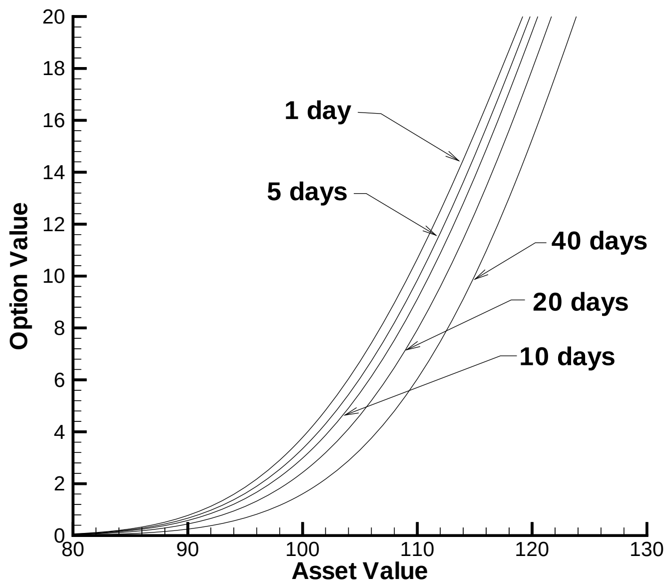

FIG. 8. *Comparison of delta and gamma of a fixed strike Asian call option with Parisian knock-in barrier for various values of J^*. $\sigma = .25$, $T - t = .5$, $r = .05$, $K = 100$, $\alpha = 2$. Asian observation frequency = 1/250 (1 day). Barrier observation frequency = 1/250 (1 day). Barrier at asset value = 120.*

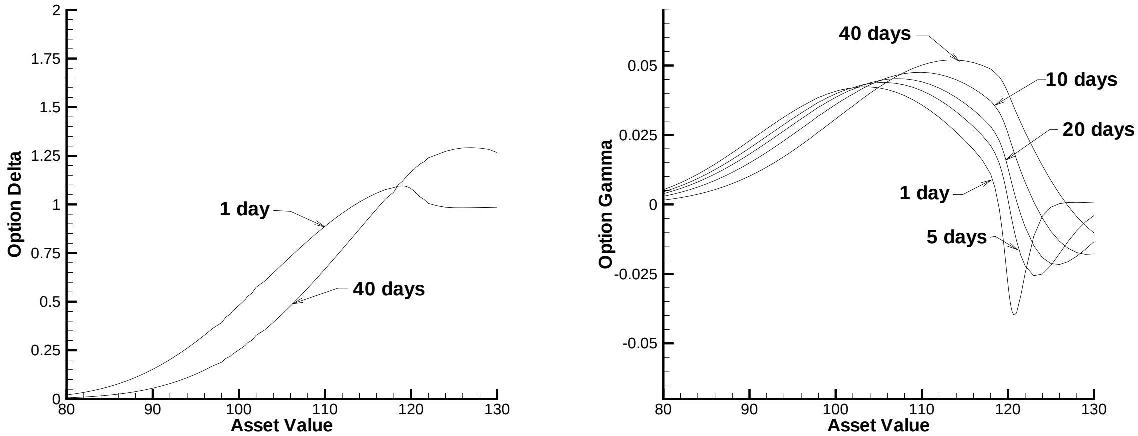

11. Knock-out barrier with CEV model. Figures 9 and 10 show the effect of different values of the CEV parameter α in equation (7), for a fixed strike Asian call with a discrete knockout barrier. In order to carry out a meaningful comparison, σ is adjusted so that the effective volatility is the same at a given price S_0 [27, 7]

$$\sigma = \sigma_{BS} S_0^{1-\alpha/2} \tag{36}$$

where σ_{BS} is the equivalent Black-Scholes volatility. In the examples shown, we use $S_0 = 100$ and values of $\alpha = 1$, 2 and 3. Clearly, these computations show that different CEV parameters can have a significant effect on the price. Larger values of α increase the effective volatility near the barrier, and hence increase the probability that the barrier will be breached. Larger values of α also reduce the maximum absolute size of delta and gamma. However, values of $\alpha < 2$ are perhaps most relevant empirically [5]. Such values are associated with higher option prices than the standard geometric Brownian motion assumption would imply. The options are also more difficult to hedge than in the usual setting.

12. Conclusion. In this article, we have described a general purpose method for pricing a wide variety of discretely monitored Asian options. Floating or fixed strike payoffs, early exercise features, and a wide variety of barrier provisions may be specified. In addition, discrete dollar dividends and a CEV process for the underlying asset can be accommodated. In particular, accurate price and hedging parameters can be obtained for discrete barriers based on the asset price and the average for the general class of Parisian barriers (which include the usual discrete barrier as a special case). Note that other types of barriers such as delayed barriers or step option type features [25, 26, 14, 34] can be easily incorporated by modifying the relevant jump conditions appropriately. Moreover, it is a simple extension to handle double barrier options.

FIG. 9. *Fixed strike Asian call option with standard discrete knock-out barrier, CEV model, various values of α. $\sigma_{BS} = .25$, $T - t = .5$, $r = .05$, $K = 100$. Asian observation frequency $= 1/250$ (1 day). Barrier observation frequency $= 1/250$ (1 day). Barrier at asset value $= 120$.*

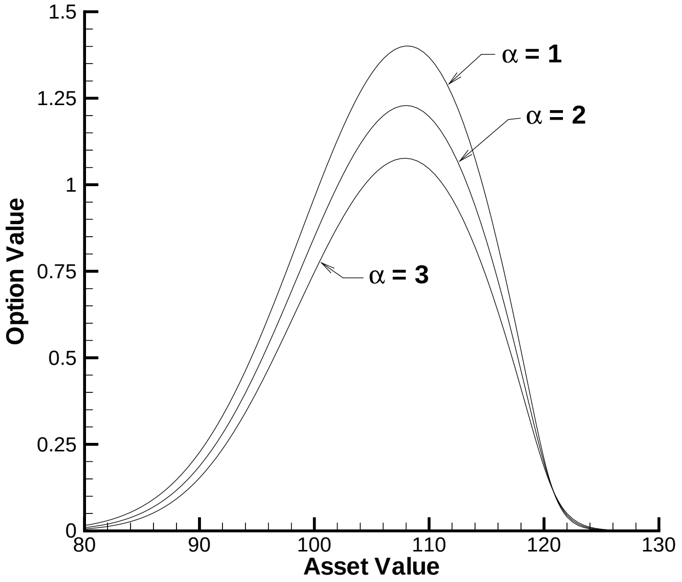

FIG. 10. *Delta and gamma of an Asian option with standard discrete knock-out barrier, CEV model, various values of α. $\sigma_{BS} = .25$, $T - t = .5$, $r = .05$, $K = 100$. Asian observation frequency $= 1/250$ (1 day). Barrier observation frequency $= 1/250$ (1 day). Barrier at asset value $= 120$.*

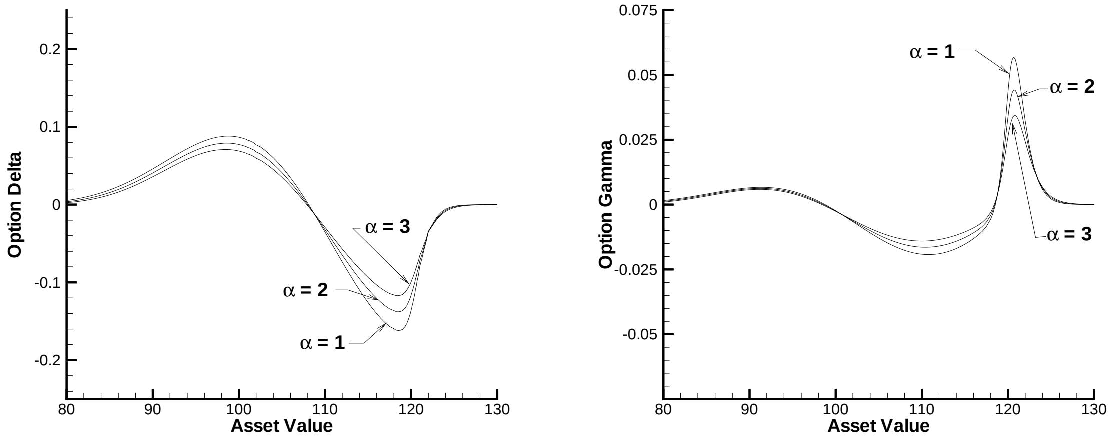

Our numerical examples suggest that:

- A formulation which uses the average as an auxiliary variable is more reliable than a method which uses the running sum, especially for American options.
- An upstream biased quadratic interpolation method for interpolating the jump conditions converges more rapidly than linear interpolation as the grid is refined.
- In some cases, reducing the observation interval from daily to one-quarter of a day can have a noticeable impact on the value of an Asian option. This indicates that a pricing method based on a continuous approximation to a discrete observation may be inappropriate in some circumstances.
- Computational time is highly dependent on required accuracy. If pricing to within 0.1% of the current asset price is acceptable, then the price, delta and gamma of virtually any type of Asian option can be determined within a few seconds on a personal computer. More accurate results require smaller mesh spacing and/or timesteps, with resulting increase in computational time.
- Various types of barriers can be used with Asian options to generate the desired price, delta and gamma characteristics. Barriers based on average values, for example, are much less sensitive to changes to underlying asset price fluctuations.
- PDE methods can be used to value Asian barrier options with any type of volatility function $\sigma = \sigma(S, t)$. Price of option contracts with barrier provisions are particularly sensitive to alternative volatility models such as CEV processes.

It is interesting to observe that pricing path-dependent contracts such as Asian or Parisian options (or mixtures of these) using auxiliary variables results in a system of independent one-dimensional PDE problems which only exchange information at observation times. In principle, this is an *embarrassingly parallel* application which could be solved extremely rapidly on existing multi-processing architectures.

REFERENCES

[1] L. Anderson and J. Andreasen. Volatility skews and extensions of the Libor market model. Working paper, General Re Financial Products, New York, 1998.

[2] W.K. Anderson, J.L. Thomas, and B. Van Leer. Comparison of finite volume flux vector splittings for the Euler equations. *AIAA Journal*, 24:1453–1460, 1986.

[3] J. Andreasen. The pricing of discretely sampled Asian and lookback options: A change of numeraire approach. *Journal of Computational Finance*, 2:5–30, Fall 1998.

[4] J. Barraquand and T. Pudet. Pricing of American path-dependent contingent claims. *Mathematical Finance*, 6:17–51, 1996.

[5] S. Beckers. The constant elasticity of variance model and its implications for option pricing. *Journal of Finance*, 35:661–673, 1980.

[6] P.P. Boyle and S.H. Lau. Bumping up against the barrier with the binomial method. *Journal of Derivatives*, 1:6–14, Summer 1994.

[7] P.P. Boyle and Y. Tian. Pricing path dependent options under a CEV process. Conference on Numerical Methods in Finance, Toronto, 1997.

[8] P.P. Boyle and Y. Tian. An explicit finite difference approach to the pricing of barrier options. *Applied Mathematical Finance*, 5:17–43, 1998.

[9] P. Chalasani, S. Jha, F. Egriboyan, and A. Varikooty. A refined binomial lattice for pricing American Asian options. 8th Annual Derivatives Securities Conference, Boston, 1998.

[10] M. Chesney, J. Cornwall, M. Jeanblanc-Picqué, G. Kentwell, and M. Yor. Parisian pricing. *Risk*, 10:77–79, January 1997.

[11] M. Chesney, M. Jeanblanc-Picqué, and M. Yor. Brownian excursions and Parisian barrier options. *Advances in Applied Probability*, 29:165–184, 1997.

[12] T.H.F. Cheuk and T.C.F. Vorst. Complex barrier options. *Journal of Derivatives*, 4:8–22, Fall 1996.

[13] J.C. Cox. The constant elasticity of variance option pricing model. *Journal of Portfolio Management*, 22:15–17, 1996.

[14] D. Davydov and V. Linetsky. Double step options. Working paper, Department of Industrial and Operations Engineering, University of Michigan, 1998.

[15] M.A.H. Dempster, J.P. Hutton, and D.G. Richards. LP valuation of exotic American options exploiting structure. *Journal of Computational Finance*, 2:61–84, Fall 1998.

[16] E. Derman, E. Ergener, and I. Kani. Static options replication. *Journal of Derivatives*, 2:78–95, Summer 1995.

[17] J.N. Dewynne and P. Wilmott. A note on average rate options with discrete sampling. *SIAM Journal on Applied Mathematics*, 55:267–277, 1995.

[18] P.A. Forsyth and H. Jiang. Nonlinear iteration methods for high speed laminar incompressible Navier-Stokes equations. *Computers & Fluids*, 26:249–268, 1997.

[19] P.A. Forsyth, K.R. Vetzal, and R. Zvan. Convergence of lattice and PDE methods for Asian options. Working paper, Department of Computer Science, University of Waterloo, `http://yoho.uwaterloo.ca/~paforsyt/lattice.ps`, 1998.

[20] J. Hull. *Options, Futures and Other Derivatives.* Prentice Hall, Third edition, 1997.

[21] J. Hull and A. White. Efficient procedures for valuing European and American path dependent options. *Journal of Derivatives*, 1:21–31, Fall 1993.

[22] R. Jarrow and S. Turnbull. *Derivative Securities.* South Western Publishing, 1996.

[23] A. Kemna and T. Vorst. A pricing method for options based on average values. *Journal of Banking and Finance*, 14:113–129, 1990.

[24] P. Lax and X-D Liu. Solution of two dimensional Riemann problems of gas dynamics by positive schemes. *SIAM Journal on Scientific Computing*, 19:319–340, 1998.

[25] V. Linetsky. Step options. *Mathematical Finance*, forthcoming, 1998.

[26] V. Linetsky. Steps to the barrier. *Risk*, 11:62–65, April 1998.

[27] J.D. MacBeth and L.J. Merville. Tests of the Black-Scholes and Cox call option valuation models. *Journal of Finance*, 35:285–300, 1980.

[28] C. Randall, E. Kant, and A. Chhabra. Using program synthesis to price derivatives. *Journal of Computational Finance*, 1:97–129, Winter 1998.

[29] P. Ritchken. On pricing barrier options. *Journal of Derivatives*, 3:19–28, Winter 1995.

[30] L. Rogers and Z. Shi. The value of an Asian option. *Journal of Applied Probability*, 32:1077–1088, 1995.

[31] J. Sidenius. Double barrier options: Valuation by path counting. *Journal of Computational Finance*, 1:63–79, Spring 1998.

[32] P.K. Sweby. High resolution schemes using flux limiters for hyperbolic conservation laws. *SIAM Journal on Numerical Analysis*, 21:995–1011, 1984.

[33] A.J.A. Unger, P.A. Forsyth, and E.A. Sudicky. Variable spatial and temporal weighting schemes for use in multi-phase compositional problems. *Advances in Water Resources*, 19:1–27, 1996.

[34] K.R. Vetzal and P.A. Forsyth. Discrete Parisian and delayed barrier options: A general numerical approach. *Advances in Futures and Options Research*, forthcoming, 1998.

[35] P. Wilmott, J. Dewynne, and S. Howison. *Option Pricing: Mathematical Models and Computation.* Oxford Financial Press, 1993.

[36] M. Yor, M. Chesney, H. Geman, and M. Jeanblanc-Picqué. Some combinations of Asian, Parisian and barrier options. In M.A.H. Dempster and S.R. Pliska, editors, *Mathematics of Derivative Securities.* Cambridge University Press, 1997.

[37] R. Zvan, P.A. Forsyth, and K.R. Vetzal. A penalty method for American options with stochastic

volatility. *Journal of Computational and Applied Mathematics*, 91:199–218, 1998.

[38] R. Zvan, P.A. Forsyth, and K.R. Vetzal. Robust numerical methods for PDE models of Asian options. *Journal of Computational Finance*, 1:39–78, Winter 1998.

[39] R. Zvan, K.R. Vetzal, and P.A. Forsyth. PDE methods for barrier options. *Journal of Economic Dynamics and Control*, forthcoming, 1998.

[40] R. Zvan, K.R. Vetzal, and P.A. Forsyth. Swing low, swing high. *Risk*, 11:71–75, March 1998.